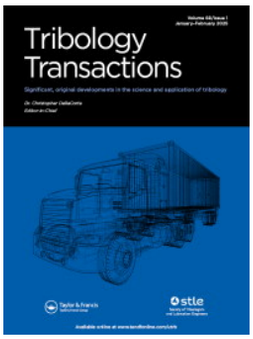

Tribology Transactions

ISSN: (Print) (Online) Journal homepage: www.tandfonline.com/journals/utrb20

Evaluation of a newly developed analytic model for predicting drag torque in wet clutches under single- and two- phase conditions using CFD

Mohammad Sadafi, Amir F. Najafi, Alireza Jalali & Robin Leister

To cite this article: Mohammad Sadafi, Amir F. Najafi, Alireza Jalali & Robin Leister (04 Mar 2025): Evaluation of a newly developed analytic model for predicting drag torque in wet clutches under single- and two- phase conditions using CFD, Tribology Transactions, DOI: 10.1080/10402004.2025.2474539

To link to this article: https://doi.org/10.1080/10402004.2025.2474539

Evaluation of a newly developed analytic model for predicting drag torque in wet clutches under single- and two- phase conditions using CFD

Mohammad Sadafi [a], Amir F. Najafi [a,*] , Alireza Jalali [a] , Robin Leister [b]

[a]School of Mechanical Engineering, College of Engineering, University of Tehran, P.O. Box 11365/4563, Tehran, Iran
[b]Institute of Fluid Mechanics, Karlsruhe Institute of Technology (KIT), 76131, Karlsruhe, Germany

*Corresponding author: E-mail address: afnajafi@ut.ac.ir (Amir F. Najafi).

ABSTRACT

The relative motion and the presence of oil between two wet clutch disks generates considerable drag torque. Aeration occurring at specific rotational speeds can effectively reduce this drag torque. This study presents a new analytical model for estimating critical speed and drag torque in radially grooved wet clutches under single- and two-phase flow conditions. Direct numerical simulation of single-phase flow confirms that the flow regime is laminar. Consequently, a validated CFD model under laminar conditions is employed to evaluate the proposed analytical model. The new model reduces deviation from numerical results by 50% compared to previous models. Furthermore, this model is extended to address the two-phase conditions, with numerical simulations confirming its accuracy within a 3% margin.

KEYWORDS: Wet clutch, Analytical solution, CFD, Drag torque, Aeration, Single- and two-phase flow.

INTRODUCTION

Increasing pollution caused by fossil fuels has led researchers to continuously seek ways to reduce fossil fuel consumption in industry and vehicles. For instance, the transmission system and clutches have a major impact on energy loss and fuel consumption. Improving device component performance and reducing power loss are effective strategies for achieving this goal. A clutch facilitates the connection and disconnection of engine power to gears during gear changes, typically comprising two parallel annular disks - one linked to the motor shaft and the other to the gear shaft. When these disks separate, it enters a disengaged mode, terminating power transmission from the motor engine to the gearbox.

Clutches can be categorized into two main types: dry and wet clutches. Wet clutches are commonly used in heavy-duty vehicles and industrial machinery such as compressors, pumps and turbines. They are also used in automatic transmissions, limited slip-differentials, and dual-clutch transmissions as the shifting element of choice. This type of clutch operates by pumping proper type of oil between two each disk when disengaged, creating shear stress that increases drag torque. This leads to energy loss and an increase in temperature within the clutch system. To improve the energy efficiency, it is important to reduce this energy loss. Previous studies show that at low rotational speeds, the clutch system operates with a single-phase oil flow (1). However, as rotational speed increases, air bubbles may penetrate the gap between disks, a phenomenon known as aeration, which occurs at a critical speed threshold. As rotational speed increases, air fills the domain. Its lower viscosity significantly reduces drag torque, leading to decreased energy loss. Drag torque is a key parameter defining clutch performance.

To clarify the flow behavior, examining well-known fluid flows can help simplify the phenomenon. The flow within the clutch can be represented as a combination of two types of flow occurring simultaneously. The first flow is similar to the Couette flow that is caused by the rotational motion of the friction disk. The second flow is similar to the Poiseuille flow and is driven by the radially pumped oil within the domain, starting from the inner radius.

As the rotational speed increases to a critical value, the radial pressure gradient resulting from the Couette-like flow starts to dominate over that from the Poiseuille-like flow. This causes air to enter the domain from the outer radius, initiates aeration. Previous studies have shown that for simple disk clutches, the critical speed tends to be quite high (2); however, creating grooves on the rotating disk can reduce this critical speed.

These grooves impart more tangential momentum to the passing oil, which increases the radial pressure gradient and facilitate smoother oil exit from the gap, leading to earlier aeration. One of the early studies on wet clutches was conducted by Kato et al (1), who developed two analytical equations for pressure distribution and drag torque in the clutch, based on the work of Hashimoto et al (3). However, their results deviated significantly from experimental results due to certain inaccurate assumptions. In this regard, Kitabayashi et al. (4) proposed an alternative analytical method for estimating the drag torque. This model is based on Couette flow conditions but considers simplifying assumptions that only support single-phase flow. They also explored the impact of various parameters, such as the number of grooves and oil flow rate, on clutch performance through experimentations. The results showed that reducing the oil flow rate or increasing the number of grooves decreases the critical speed. Yuan et al. (5) developed a more accurate analytical model by considering the influence of surface tension in the flow equations. However, the predictions still differed significantly from experimental results. Fluid flow in a

non-grooved clutch was simulated using ANSYS-FLUENT, and including surface tension in the simulation helped reduce the deviation between numerical and experimental results. Iqbal et al. (6) introduced an analytical model for the drag torque estimation that included the effect of cavitation, but they could not confirm cavitation in the clutch experimentally. Wu et al. (7) conducted an experimental and numerical investigation on a grooved wet clutch under single- and two-phase conditions, accounting for the effect of axial force on the stationary disk. Guo et al. (8) carried out a numerical study on a non-grooved wet clutch, analyzing the simultaneous motion of both disks in the same and opposite directions. Their findings emphasized the significant effects of simultaneous disk motion on drag torque, critical speed, and phase distribution in multiphase flow. It was also shown that drag torque increases substantially when the two disks rotate in opposite directions.

Wang et al. (9) focused on key parameters in numerical simulations, such as iteration number, convergence criteria, initial and boundary conditions, providing valuable insights for researchers in this field. Neupert et al. (10) conducted a comprehensive experimental study on wet clutches, exploring the influence of various parameters like gap height, groove dimensions, flow rate, and groove patterns on clutch performance. They compared their experimental findings with analytical models and performed numerical simulations using ANSYS-Fluent employing a high-resolution mesh and considering the surface tension and temperature variations (11). In the following, they investigated a special groove pattern combining parallel and waffle-shaped grooves and showed better performance than simple radial grooves."

Pahlovy et al. (12) proposed an analytical model to predict drag torque and aeration onset in single- and two-phase conditions. While the model performed satisfactorily in the single-phase region, the results in two-phase flow deviated significantly from experiments.

Leister et al. (13) derived simplified governing equations for fluid flow within wet clutches using order-of-magnitude analysis and introduced a new dimensionless number. This number analytically suggests the critical speed for aeration onset. They also developed a new analytical model that addresses the limitations of Pahlovy's model (12), using the concept of hydraulic diameter. In another study, Leister et al. (14) conducted experimental research using the defocusing particle tracking velocimetry (DPTV) method to examine the flow behavior in different sections of a radially-grooved clutch. The results were highly accurate and can be useful for thoroughly understanding the flow domain. Their latest study includes the derivation of simplified governing equations that consider the effect of gravity (15).

Sax et al. (16) investigated the flow topology in the grooved wet clutch with 6 different radial groove patterns. They provided the radial, axial, and tangential velocity contours of the fluid in the grooved region obtained by experiments and compared the experiments with the CFD results. However, their work contains little information about the methods for estimating the drag torque value.

Zhang et al. (17) proposed a hybrid model combining a previously presented analytical model earlier (18) and a Particle Swarm Optimization-Back Propagation (PSO-BP) neural network to overcome the limitations of the analytical model in drag torque estimation. Their results showed better agreement with the experiments compared to the analytical results. Nevertheless, the structure of the proposed model has not been clearly described and does not provide good insight into the effects of varying different parameters on the value of the drag torque.

Pointner-Gabriel et al. (19) developed a method to create a data-driven model to estimate the drag torque in the wet clutch and described the model and results in detail in their recent work (20). They created a dataset based on the results of a test rig and used a corresponding machine

learning algorithm to establish relationships between the various parameters that influence drag torque. Ultimately, the model predicts the drag torque as a function of rotational speed. The results of this study are a step forward in the estimation of the drag torque, as they avoid the computational costs of numerical studies and the economic costs of experimental studies. However, due to the limited amount of data on which the model was trained, the results may not be reliable for all types of wet clutches. Furthermore, the effect of the geometrical parameters was not considered in the extracted model.

Previous studies have examined a wide range of effective parameters on the performance of wet clutches. However, there are still shortcomings that require further investigation. For instance, those studies did not focus on the type of fluid flow regime in the clutch. It is noteworthy that choosing the appropriate fluid flow regime is important for the accuracy of simulation results.

In addition, differences between the results of the analytical models and the experimental data persist due to the geometric complexity caused by the presence of grooves and the challenges in analytically solving two-phase flow equations. Moreover, performing experiments or CFD methods for practical problems is often inefficient due to the high economic and time costs. Newer data-driven models allow fast and precise measurement of the drag torque. However, they are not yet advanced enough to account for the effects of individual geometric parameters -such as width and depth of the grooves in the radial pattern-on clutch performance. To address these shortcomings, the present work investigates a new analytical model, evaluates its accuracy and extends it to cover the two-phase condition and estimates the critical speed and drag torque. This analytical model can account for the effects of different geometrical parameters in estimating the drag torque with reasonable accuracy.

In the first step, an attempt will be made to determine the type of flow passing through the wet clutch using the direct numerical simulation (DNS). DNS is conducted using NEK5000 software, with results validated by experiments from Neupert et al. (10) and Leister et al. (14). This process investigates the possibility of turbulence in the flow field. The findings show that the flow regime in this type of clutch is laminar, based on the stabilization of velocity variations over time.

Afterward, a steady-state laminar flow simulation is performed using the OpenFOAM solver to ensure that there are no differences between the DNS and laminar simulation results. Subsequently, this validated CFD model is used to investigate the performance of an analytical model for drag torque prediction under single-phase conditions. Finally, a mathematical analysis is performed to extend the analytical model to predict drag torque under two-phase flow conditions. The CFD results evaluate the analytical estimates and show reasonable agreement.

GEOMETRICAL DESCRIPTION AND COMPUTATIONAL DOMAIN

The basic geometry of the wet clutch with radial grooves, including the most important geometric parameters and boundary conditions, is shown in Fig. 1. The grooved disk acts as a rotating component, while the non-grooved disk remains stationary.

The geometrical parameters of two clutches are listed in

Table ***1***. The first Case refers to an experimental study conducted by Leister et al. (14), while the second Case is based on the research done by Neupert et al. (10), chosen for its available experimental data on two-phase flow.

To reduce the computational costs and time, a fraction (1/32) of the entire clutch is simulated in Case 1, employing periodic boundary conditions on the left and right sides. In Case 2, a similar approach is chosen, where only 1/60 of the entire clutch is modeled. The grooved disk rotates at a constant rotational speed, ω. The radial flow is pumped from the inner radius, R_1, with a constant volumetric flow rate, Q, into the clearance between the two disks and exit at the outer radius, R_2.

NUMERICAL SIMULATION

Governing Equations

In order to solve fluid flow problems, at least two equations must be considered: the continuity equation and the Navier-Stokes equations. These equations, which are used for single-phase flow problems, are as follows:

$$\frac{D\rho}{Dt} + \rho\,\nabla\vec{U} = 0 \qquad (1)$$

$$\rho\,\frac{D\vec{U}}{Dt} = \rho\vec{g} - \nabla P + \nabla\cdot(\mu\nabla\vec{U}) \qquad (2)$$

where ρ is the density, t is the time, $\vec{U}$ denotes the velocity vector, μ is the dynamic viscosity, P is the pressure, λ is the coefficient of bulk viscosity, and $\vec{g}$ is the gravitational acceleration.

Previous experiments have demonstrated that the distribution of phases in two-phase flow is highly non-uniform, characterized by distinct air bubbles (11). To analyze this multiphase flow, the volume of fluid (VOF) model is used, which taken into account surface tension to capture the

interfaces between the two immiscible fluids. The use of the VOF method in the model effectively depicts the entire aeration process, as has been observed in some previous experiments (7,11).

Since the interfaces move into the flow domain and the phase distribution changes rapidly, the flow cannot be considered stationary over time. Therefore, a transient simulation is necessary to be conducted. In transient simulation, it is crucial that the time-steps are sufficiently small to stabilize the simulation results. In this method, a volume fraction, α, is defined for each phase, which represents the ratio of the volume of this phase within a computational cell to the total volume of the cell. The sum of the volume fractions for all phases within each computational cell must be equal to one. In this case, this can be expressed as follows:

$$\alpha_{oil} + \alpha_{air} = 1 \quad (3)$$

The VOF model solves a single momentum equation and a single continuity equation. The density and viscosity terms in these equations are defined with the volume fractions of both phases, as shown below:

$$\rho = \alpha_{oil}\rho_{oil} + \alpha_{air}\rho_{air} \quad (4)$$

$$\mu = \alpha_{oil}\mu_{oil} + \alpha_{air}\mu_{air} \quad (5)$$

As a result, only a single velocity field is obtained that directly couples the phases at the interface. To track the phase interface, the continuity equation is solved again using the volume fraction of one phase, as follows:

$$\frac{\partial(\alpha_{oil}\rho_{oil})}{\partial t} + \nabla \cdot \left(\alpha_{oil}\rho_{oil}\vec{U}\right) = 0 \quad (6)$$

The volume fraction of the other phase is obtained from Equation (3). By solving the continuity and momentum equations using the VOF model, the velocity and pressure distributions of the fluid mixture, as well as the volume fraction of each phase, are determined. Two methods are used to perform numerical simulations: steady-state laminar flow and DNS. In the DNS approach, the goal is to capture all structures and characteristics of the flow on all scales and at all time steps. Although DNS provides a detailed and accurate representation of the flow field, it is computationally expensive. The challenges of DNS include the choice of temporal and spatial discretization methods, minimizing numerical errors, determining the appropriate grid size, and ensuring sufficient computing resources. According to Kolmogorov theory, which describes the size of the smallest eddies in turbulent flows, the smallest element in the computational grid should be of the order of the Kolmogorov scale (21). As a result, the number of elements required for an isotropic homogeneous turbulent flow problem is approximated by $N \approx 4 \cdot 4\, Re_L^{\frac{9}{4}}$, where Re_L represents the turbulent Reynolds number defined as $k^{1/2}L/v$, and L is the characteristic length of the flow. Wilcox et al. (22) presented $N \approx (3Re_\tau)^{\frac{9}{4}}$ for the cavity flow problem, where $Re_\tau = u_\tau H/(2v)$, H is the cavity width, and $u_\tau \approx U_m/20$. It is noteworthy that all these equations were derived for a specific problem, raising doubts about their applicability to different types of fluid flow problems. As the Reynolds number increases, turbulent effects in the flow also increase, so that a smaller computational grid size is required. For this reason, DNS has so far been limited to low and medium Reynolds numbers.

CFD solvers

Two different CFD codes were used for numerical simulations. NEK5000 is an open-source code based on the spectral element method (SEM) for spatial discretization. SEM combines the accuracy and rapid convergence of spectral methods with the flexibility of the finite element

method. As a result, SEM is often chosen as the discretization method for DNS. The details of this method are beyond the scope of this study and are presented in (23) . NEK5000 facilitates DNS, which is essential for obtaining accurate numerical results, especially for fully turbulent flows. The DNS was performed to achieve an accurate and reliable solution of the fluid flow in the wet clutch for further investigation of the flow regime. The other CFD code used in this work is OpenFOAM, which is also open-source and is based on finite volume discretization. OpenFOAM was used for modeling steady-state laminar simulations of fluid flows due to its simplicity and flexibility.

Boundary conditions

A fixed volumetric flow rate is chosen for the inlet boundary, with a gauge pressure of zero ($P_{gauge} = 0$) at the outlet. The grooved disk is subject to a moving wall boundary condition with a constant rotational speed, while the non-grooved disk is treated as a stationary wall with a no-slip condition. The presence of grooves makes it difficult to apply rotational speed to the friction disk, since the groove sidewalls are oriented perpendicular to the direction of rotation. Applying the rotation to these sidewalls requires the use of dynamic meshes, which increases both computational cost and complexity. Alternatively, the multiple reference frame (MRF) model can be used. In this model, the grooved disk remains stationary while the non-grooved disk rotates in the opposite direction. Thus, the desired rotation is achieved by positively rotating the entire reference frame using the MRF model. The boundary conditions are depicted in Fig. 2.

In the two-phase simulations based on the VOF model, the volume fraction of the oil at the inlet is set to one, which indicates a pure oil in-flow. At the outlet boundary, the oil exits as a free jet due to the high rotational speed, while the air is drawn into the flow domain due to a positive radial pressure gradient near the outlet, caused by the centrifugal force. Hence, the volume

fraction of the backflow oil is designated as zero, symbolizing the penetration of air into the domain. This is achieved by setting the "InletOutlet" boundary condition for the volume fraction at the outlet boundary. The initial condition for the volume fraction of the oil is set to 0.8 in order to achieve faster convergence.

Mesh generation

To ensure the accuracy and convergence of the simulation results, three-dimensional hexahedral meshes are generated for all cases. For the steady-state laminar simulations in OpenFOAM, the structured mesh has been generated using the commercial software ANSYS ICEM-CFD with approximately 1.5×10^6 hexahedral cells. Fig. 3. Computational gridshows the computational grids. To study the independence of the solution from the mesh, three different meshes were used, containing 4.8×10^4, 7×10^5, and 1.5×10^6 cells. The drag torque value on the stationary disk was considered as the output parameter. The variation in drag torque across the three meshes was less than 2%, which confirms that the results are not significantly affected by the grid size. For the DNS cases of the NEK5000, the size of the elements must be fine enough to capture the smallest eddies that exist in the flow. There is no general criterion to determine the number of elements or the appropriate size of elements required to perform DNS for different flow problems. Most studies refer to Ref. (21), which suggests the number of elements as a function of Re_λ required for obtaining homogenous isotropic turbulence. However, this relationship is specific to a particular problem and cannot be generally applied to different flows. Nevertheless, following the practice applied to the DNS of rotating cavity flows, (e.g. (24-27)), four 3D meshes with 1.8×10^6, 2.8×10^6, 8.2×10^6, and 1.03×10^7 cells were generated to study the independence of the solution from the mesh size. Again, the drag torque value on the stationary disk was considered

as the output parameter. The change in drag torque between the two finest meshes was 2.3%, indicating that the calculated results are independent of the grid size.

Time-stepping and convergence criteria

OpenFOAM can solve both the steady-state and transient problems. For the single-phase cases in OpenFOAM, the SimpleFoam solver was used, which is a steady-state solver based on the SIMPLE algorithm. For the multiphase cases, the InterFoam solver was utilized, which solves two-phase flow problems over time using the VOF model and the SIMPLE algorithm. To maintain stability in transient simulations, the Courant-Friedrichs–Lewy (CFL) number should generally be kept below one. To achieve this, the time step value should be set to a very small value, especially since the element sizes are also very small. The initial time step was set to 10^{-5} s, and the variable time-stepping mode was enabled to automatically maintain the CFL limit. The CPU model used for the simulations is Intel(R) Xeon(R) E5-2696 v4. The number of CPU cores used for the OpenFOAM simulations was 16, and the computation time for each simulation was approximately 24 hours to meet the convergence criteria.

The convergence criterion was set to ensure that the L_2-norm of residuals is less than 5×10^{-5} for single-phase flows and 10^{-4} for two-phase flows in all the governing equations. It is well known that DNS cannot be assumed stationary in time. This is because the goal of DNS is to capture all spatial and temporal characteristics of the flow without any simplifying assumptions or modeling. Thus, all cases related to NEK5000 are time-dependent. Given the large number of cells and their small size, the appropriate time step for this case is about 10^{-8} s, which imposes a huge computational cost. Therefore, the operator integration factor scheme (OIFS) module of NEK5000 was used, which allows the target CFL number of the simulation to be increased up to

4 without causing divergence or instability. With the application of OIFS, the time step value could be increased up to 10^{-6}. The number of CPU cores used to perform the DNS simulations was 60, corresponding to the large amount of computational grids, and each simulation took about 7-10 days.

In NEK5000 simulations, the residual tolerances were set to 10^{-6} and 10^{-8} for pressure and velocity. Transient simulations were performed until the drag torque on the stationary disk and the average of oil volume fraction in the whole domain reached a constant value in terms of time.

RESULTS AND DISCUSSION

In this section, numerical and analytical results for fluid flow in wet clutches under both single-phase and two-phase flow conditions are presented and discussed. The main objective is to develop a novel analytical model that can estimate the drag torque and critical speed in the whole range of clutch rotational speed with reasonable accuracy. To achieve this, a reliable CFD model is needed to evaluate the analytical results.

Single-phase flow condition

In this section, at first the results of the CFD simulations are validated by comparison with existing experimental data. Subsequently, DNS simulations are performed to obtain accurate results and determine the flow regime based on the presence of the velocity fluctuations in terms of time. Confirming the laminar regime for the flow, a steady-state laminar CFD model is then used to evaluate the accuracy of the analytical model proposed by Leister et al. (13), in comparison to the earlier model (12).

CFD model validation

For the single-phase simulations, the geometry of Case 1 introduced in

Table ***1*** is generated, and the results are compared with experimental data. **Error! Reference source not found.** displays the non-dimensionalized tangential velocity contours in the grooved and non-grooved areas of the clutch. The contours are based both on experimental observations and on the numerical results of the DNS and OpenFOAM simulations of the laminar flow. In the experimental data, a region of high-velocity can be seen in the center of the grooved region, which is also present in the numerical results. Furthermore, both the experimental and numerical results demonstrate a linear change in velocity magnitude from one disk to another in the non-grooved region, which is similar to a Couette-type flow.

A comparison between the experimental and numerical wall shear stress can also be made to better understand the flow regimes and their effects on clutch performance. **Error! Reference source not found.** shows the comparison of the numerical and experimental results for the non-dimensionalized wall shear stress, which is given as $\tau_{w,lin} = \mu R_m \, \omega / h$ in the grooved region.

Error! Reference source not found.a shows that the comparison between the numerical and experimental results is satisfactory, with a maximum difference of about 6%. As one can see, both curves drop slightly in the circumferential direction. Similarly, **Error! Reference source not found.**b shows good agreement between the numerical and experimental results with a maximum deviation of about 3%, which is within an acceptable error range.

Fig. 6 illustrates the non-dimensionalized tangential velocity obtained by the steady-state laminar simulation in OpenFOAM and its comparison with experiment (14) across the non-dimensionalized axial direction at the center of the groove, where $\frac{\theta R_m}{W} = 0.5$. It is obvious that the numerical and experimental data coincide, showing no significant difference between them.

DNS and laminar simulations

After validating the DNS simulation with the experimental results and ensuring that the numerical results are in good agreement with the experimental results, the DNS simulation was performed for the fluid flow in the wet clutch (Case 1 in

Table ***1***) at two rotational speeds of 23 and 80 rad/s. DNS provides the most accurate results for the flow characteristics, regardless of the flow regime. The choice of these two speeds is based on the fact that the critical speed for this case, as will be discussed later, is 85 rad/s, and choice of 80 rad/s as a higher value assists in examining the entire single-phase region.

Most previous studies that focused on numerical simulation of flow in wet clutches assumed a laminar flow regime (9, 12, 13). However, none of them has thoroughly investigated whether their assumption is correct or incorrect, which is crucial for a comprehensive understanding of flow physics in open clutch. The best-known characteristic of a turbulent flow is that the velocity and pressure of the fluid in a turbulent flow are subject to irregular fluctuations in magnitude and direction. Therefore, turbulence is inherently chaotic and unpredictable. Turbulence models attempt to capture the essential characteristic of turbulence in a deterministic way based on the flow governing equation. In DNS however, there is no turbulence modeling and the smallest temporal and spatial scales of the flow are solved directly. As a result, any turbulence in the flow can be identified in the temporal fluctuation of velocity or pressure. Conversely, if the velocity and pressure at different points of the flow domain reach a constant value with respect to time and are stable, it can be concluded that there is no turbulence in the flow.

Fig. 7. Variation of velocity magnitude in 4 arbitrary locations in terms of shows the variation of velocity magnitude at four arbitrary locations in terms of time obtained from DNS simulation at $\omega = 80\ rad/s$. The locations where the velocity magnitude is obtained are at $R_m = \frac{R_1+R_2}{2} = 0.0881\ m$ and $\theta = 2°, 4°, 8°, and\ 10°$, at $\frac{Z}{h} = 0.5$. It is obvious that the velocity magnitude varies at first, but after about 2×10^{-3}s, it stabilizes and reaches a constant value in all four graphs. Similar results are obtained for the pressure value. Therefore, no turbulence can be seen in the DNS results.

In the following, a steady-state laminar simulation is performed for the two conditions mentioned above using OpenFOAM, and the results are compared with the DNS results. This is to ensure that there is no difference between the DNS and steady-state laminar results and validating the laminar regime assumption for the following studies. To compare the results of both cases, an approach described in Refs. (28-31) is to select a key parameter that is directly affected by the flow physics and compare its values at similar locations. In this study, the wall shear stress and drag torque are chosen as comparable parameters.

Table 2 displays the details of the individual simulations and the measured drag torque on the stationary disk for each case. The calculated drag torque for laminar and DNS cases differs only by 0.001 N.m, which is negligible.

Fig. 8 demonstrates the non-dimensionalized wall shear stress along the clutch radius for $\omega = 80$ rad/s, at different angular positions (taking into account the angular direction shown in Fig. 1b). Based on the simulations of the two-phase flow simulations presented in section 4.2.2, the critical speed in this case is $\omega_c = 85$ rad/s. Comparing the laminar and DNS results in Fig. 8a and Fig. 8d, there is no noticeable difference between the two, the curves follow each other closely. In Fig. 8b and Fig. 8c, however, some discrepancies can be observed in certain regions (around $R = 0.084\,mm$ to $R = 0.086\,mm$). These discrepancies are particularly noticeable at $\theta = 4^{\circ}$ and $\theta = 8^{\circ}$ near the grooves. The wall shear stress is constant in the Couette flow along the wall (here in the tangential direction) and depends on the pressure gradient in the Poiseuille flow. In the clutch, the radial flow of the oil behaves similarly to the Poiseuille flow at the domain inlet so the wall shear stress varies considerably. At higher radii, the dominant flow behavior shifts towards Couette flow due to the increase in the centrifugal momentum of the flow -caused by the increase in radius- so that the value of the wall shear stress becomes

independent of the pressure gradient and only varies linearly with the radius. This leads to a decreasing gradient of the wall shear stress curve. The graphs clearly show that the value of the dimensionless drag torque varies so slightly and remains almost constant for radii above 0.085 m, which indicates a pure Couette flow.

Based on this description, the DNS results in Fig. 8b and Fig. 8c are consistent with the flow physics and the sudden peak in the laminar simulation results could be due to modeling and/or numerical errors. Consequently, it can be deduced again that the flow regime is laminar throughout the range of rotational speed in which the flow is single-phase (from 0 to 80 rad/s). Therefore, this validated CFD setup with laminar flow can be used for the following investigations. Finally, it should be noted that the general method for determining the flow regime is based on the value of the Reynolds number. If the Reynolds number, similar to the flow in the channel (Poiseuille flow) and based on the hydraulic diameter, is defined as equation (7):

$$Re_{\mathrm{h}} = \frac{R_2 \omega h_{eq}}{\nu} \qquad (7)$$

Re_h for the two cases is 26.4 and 91.7, which are both small and indicate that the flow regime is predominantly laminar over the entire range of rotational speeds. Moreover, in Ref. (32), it was found that for flows in rotor-stator cavities, $Re_r = 8 \times 10^5$ is the beginning of the flow transition from laminar to turbulence. Moreover, Dmitrenko (33) presented a solution for the critical Reynolds number near a rotating disk based on the stochastic equations of the continuum laws and the equivalence of measures between random and deterministic motions. They argued that the critical Reynolds number is $3.25 \times 10^5 \leq Re_{cr} \leq 7.3 \times 10^6$ based on some assumptions.

It is important to clarify that these conclusions refers to a single rotating disk in an infinite fluid, not to a system of rotor and stator. Also, as claimed in Ref. (34), the initial breakdown of laminar flow in a system of rotor and stator occurs around $Re_{cr} \approx 2 \times 10^5$, which has been also confirmed implicitly in Ref. (35). While there is considerable discrepancy in the suggested values for the transitional Reynolds number in the different references, adopting any of these values as the criteria leads us to assume laminar flow in the present cases. This assumption is based on the fact that the highest rotational Reynolds number (Considering R_2 as characteristic length) examined in this study is 14,320.

Evaluation of the analytical model performance in single-phase condition

As already described, the use of radial grooves in open wet clutches has a significant influence on the clutch performance. Studies have shown that the presence of these grooves increases aeration and reduces the critical speed (10). Various analytical methods for predicting drag torque and pressure gradient distribution have been proposed in literature, but they are often unable to accurately predict the behavior of grooved clutches (2, 6, 7)

The presence of grooves causes non-smooth geometry and additional complexity in the flow physics, which makes the prediction of flow properties with analytical approaches extremely difficult. One approach, as outlined by Pahlovy et al. (12), explicitly models the grooves by introducing an equivalent gap height ratio for the grooved disks.

$$h_{\text{eq,Pahlovy}} = h + H\, a_g = h + H \frac{A_{groove}}{A_{disk}} \quad (8)$$

Based on this analytical approach, the drag torque is obtained as:

$$T = \frac{\pi \mu \omega}{2 h_{eq}} \left({R_2}^4 - {R_1}^4 \right) \quad (9)$$

where h has been replaced by h_{eq}. Although this approach agrees partially with some numerical and experimental data, Leister et al. (13) have demonstrated that this model has weakness in predicting drag torque, especially when there are variations in the geometrical parameters of the disks and grooves. Their new approach is based on concept of the hydraulic diameter, a common method for simplifying complex geometries in fluid mechanics. Based on this concept, the equivalent gap height was introduced as follows:

$$h_{\mathrm{eq}} = \frac{D_h}{2} = \frac{2A}{p} = \frac{h\pi(R_1+R_2)+nHW}{\pi(R_1+R_2)+nH} \tag{10}$$

The investigation indicates that this model performs better than the earlier model of Pahlovy et al. (12). However, further experiments and calculations are necessary to obtain a more accurate conclusion. It is important to note that the model has not been validated with experimental or numerical data. . Further research is required to thoroughly investigate the effect of geometric features, such as the height and width of the groove, to gain a more comprehensive and accurate understanding. Having established a validated and accurate CFD model for the simulation of fluid flow with the laminar regime in the previous section, several simulations are performed for Case 1 to investigate the accuracy of the new analytical model under single-phase conditions. This is done by varying the gap height, the groove height and the groove width and compare the simulation results with the two analytical models.

Fig. 9a displays the changes in dimensionless drag torque resulted from the simulation and the two aforementioned models as the gap height changes. The drag torque is non-dimensionalized by the maximum value obtained in the simulations. The rotational speed is set to 30 rad/s and the groove height and width to 0.97 and 1.35 mm, respectively. The drag torque decreases with increasing gap height. This is comparable to the behavior of the shear stress in the Couette flow when the gap between the two plates increases. It can be seen that the drag torque estimated by

both analytical models deviates significantly from the numerical results at smaller gap heights. The maximum deviation is around 27%, at $h = 200\ \mu m$, which represents a considerable difference. From $h = 500\ \mu m$, however, the numerical and analytical data align.

When comparing the two analytical models, the predicted values are close to each other, although the model for the hydraulic diameter is slightly more accurate. The analytical groove models are therefore more suitable for larger gap heights.

Fig. 9b illustrates how the dimensionless drag torque changes with the groove depth. The drag torque is non-dimensionalized by the drag torque of a non-grooved clutch. The rotational speed is set to 30 rad/s and the gap height and groove width are set to 0.6 mm and 1.35 mm, respectively. It is obvious that an increase in the groove height and i.e. an increase in the cross-sectional area of the groove has a favorable effect on the drag torque, as the oil flow is facilitated radially and the oil exits the gap between the two disks more quickly. The deviation of the hydraulic diameter model from the numerical results is about 50% less than with the previous model (12).

This is also evident in Fig. 9c, which shows the variation of the dimensionless drag torque in terms of the groove width. The maximum differences between the numerical data and hydraulic diameter model in these cases are 8.2% and 7.1%, respectively. The CFD results suggest a gradual decrease in drag torque in terms of groove depth and width, while analytical curves (for both models) decrease linearly with a steeper slope. The formula for the equivalent gap of the hydraulic diameter model improves the prediction of drag torque value in comparison to Pahlovy model (12). With increasing gap width and depth, the difference between the numerical and analytical results increases, but it should be noted that the practical values of the groove depth and width do not exceed the intended values.

Fig. 9d shows the dimensionless drag torque values for the condition, in which the rectangular cross-sectional area of the groove is constant ($HW = 1.31\ mm^2$), while the values of H and W vary. The drag torque is non-dimensionalized by the drag torque of a non-grooved clutch. The horizontal axis of this diagram is the aspect ratio of the grooves (H/W). It can be seen that the Pahlovy model (12) does not capture the variation of the aspect ratio, while the hydraulic diameter model captures this variation and as the aspect ratio increases, the experimental and numerical values converge.

It seems that due to the definition of h_{eq} in Pahlovy model, Equation (8), the effect of groove height (H) dominates the other variables in the calculation of h_{eq} because it is multiplied by the area ratio (A_{groove}/A_{disk}), which may not be sufficiently consistent with the physics of the flow, and it causes the deviation of analytical results from the numerical results. In the hydraulic diameter model, h_{eq} is a function of h, W, and H. In contrast to the model of Pahlovy et al. (12), the hydraulic diameter model considers all geometric variables and thus provide more accurate results. Further modifications of this model in the following investigations could improve its predictive capabilities.

Two-phase flow condition

As previously described, aeration, which decreases the drag torque on the stationary disk, starts at a certain rotational speed. Under this condition, the flow within the domain is two-phase.
To analyze the flow characteristics of a multiphase flow, experiments, analytical models and numerical simulations can be utilized. However, the existing analytical models are not enough accurate in predicting the drag torque in the two-phase conditions, and the hydraulic diameter model has not been derived for two-phase conditions at all. Furthermore, numerical simulation is not efficient for the computation of drag torque and critical speed in engineering applications,

due to the high computational cost and time-consuming nature of multiphase simulations. The hydraulic diameter model has shown acceptable accuracy in predicting the drag torque in single-phase conditions. Therefore, in this section, after creating a two-phase flow simulation model using OpenFOAM, the hydraulic diameter model is generalized to cover the two-phase condition employing a simplifying assumption and mathematical operation, and the results are compared with numerical results and show good agreement. Moreover, the analytical estimation of the critical speed is evaluated by comparison with the results of the CFD model.

CFD model validation

To validate the two-phase simulations carried out by OpenFOAM, a comparison was conducted between the numerical results and the experimental data from Neupert et al. study (10) in identical conditions. The geometrical parameters are those listed in Table 2 as Case 2. **Error! Reference source not found.** illustrates the drag torque in terms of rotational speed for both the experimental and numerical results. As can be seen, the numerical results are in good agreement with the experimental results. It should be noted that the critical speed computed by the numerical approach is $\omega_c = 860\ rpm$, which is 3.5% different from the value measured by the experiment, $\omega_c = 830\ rpm$.

Hydraulic diameter model generalization

Leister et al. (13) simplified the flow equation based on an order-of-magnitude analysis and provided an explicit formula for calculating the radial pressure gradient in the domain:

$$\frac{dp}{dr} = -\frac{6\mu Q}{\pi h^3 r} + \frac{3\rho r\omega^2}{10} \quad (11)$$

Given the good accuracy of the hydraulic diameter model for estimating the drag torque value in single-phase flow condition, the approach of Pahlovy et al. (12) is used to generalize the hydraulic diameter model to cover the two-phase flow condition. By defining the volume

fraction of the fluid as α and introducing a critical radius, r_0, it is assumed that the flow domain from R_1 to r_0 is filled with oil and from r_0 to R_2 with air. Although this assumption lacks physical accuracy, it helps in simplifying the equations and mathematical calculations. According to this assumption, α is defined as:

$$\alpha = \frac{r_0^2 - R_1^2}{R_2^2 - R_1^2} \tag{12}$$

Integrating equation (11) yields:

$$P(r) - P(R_1) = -\frac{6\mu Q}{\pi h^3} Ln\left(\frac{r}{R_1}\right) + \frac{3\rho\omega^2}{20}\left(r^2 - {R_1}^2\right) \tag{13}$$

At the interface of air and oil, there should be a pressure drop. If the inner and outer boundary of critical radius, r_0, is shown by ${r_0}^+$ and ${r_0}^-$, the pressure drop can be written as:

$$\mathrm{P}({r_0}^+) - \mathrm{P}({r_0}^-) = \frac{2\sigma cos\varphi}{h} \tag{14}$$

where σ is the surface tension and φ is the contact angle. Based on Equation (13):

$$P(r_0^-) - P(R_1) = -\frac{6\mu Q}{\pi h^3} Ln\left(\frac{r_0^-}{R_1}\right) + \frac{3\rho\omega^2}{20}\left(r_0^{-2} - {R_1}^2\right) \tag{15}$$

Substituting Equation (14) into Equation (15) gives:

$$P(r_0^+) - P(R_1) = -\frac{6\mu Q}{\pi h^3} Ln\left(\frac{r_0^-}{R_1}\right) + \frac{3\rho\omega^2}{20}\left(r_0^{-2} - {R_1}^2\right) - \frac{2\sigma cos\varphi}{h} \tag{16}$$

The surface tension coefficient for the interface of air and oil is given as (10):

$$\sigma = -8.444 \times 10^{-5}\vartheta_{oil} + 0.02992 \tag{17}$$

where ϑ_{oil} is the temperature of the oil and taken at 30℃. Pahlovy et al. (12) mentioned that in the equilibrium condition, the pressure at the beginning of the air layer is equal to the pressure at the entry of the flow domain. Regarding this assumption, the left-hand side of equation (16),

should be equal to zero. If it is assumed that the value of r_0^- is approximately equal to r_0, the critical radius can be obtained. Computing the oil volume fraction from equation (12) and multiplying that by equation (9) provides the analytical value for the drag torque value as:

$$T = \frac{\alpha\pi\mu\omega}{2h_{eq}} \left({R_2}^4 - {R_1}^4\right) \quad (18)$$

This analysis is described in more detail in the Appendix. Once the equations are derived, several numerical simulations are performed to evaluate the accuracy of the obtained equations.

Fig. 11a illustrates the contours of the oil volume fraction for $\omega = 100\ rad/s$, and $Q = 1\ L/min$ during the simulation time. These contours highlight the dominance of the air phase over the oil phase in the clutch. As the simulation time passes, the air phase extends and the oil phase shrinks. Fig. 11b presents the drag torque as a function of rotational speed, which was obtained from CFD simulations and equation (18) at flow rates of $Q = 1, 3$ and $5\ L/min$.

The numerical and analytical results show good agreement, with a minor discrepancy at the start of the two-phase region attributed to the divergence in critical speed estimation. This discrepancy, amounting to around 3%, can be considered negligible.

Additionally, a significant difference can be observed at $\omega = 140\ rad/s$ for $\mathrm{Q} = 5\ \mathrm{L/min}$, which is probably caused by some inconsistent initial conditions. Consequently, this approach is proposed as an extension of the hydraulic diameter model for the two-phase flow, and can be used in future studies to estimate the drag torque across the entire operation range of the wet clutch, either single-phase or multiphase.

Table 3 provides the critical angular speeds estimated with equation (11) and the values obtained from CFD simulations. It is important to note that, after the start of aeration, the pressure at the

outer diameter of the clutch is lower than the ambient pressure due to an inverse pressure gradient.

By defining the other parameters, the critical rotational speed is obtained analytically by setting equation (11) to zero. The difference between the values at $Q = 1\ L/min$ is considerable, amounting to 20%; however, this difference decreases at higher flow rates. This occurs because higher flow rates fill the domain capacity more quickly, resulting in improved and faster convergence in numerical simulations. The difference between the values in the other two cases are sufficiently small.

CONCLUSIONS

The present study focuses on a new analytical model called "hydraulic diameter model" for predicting the drag torque in a grooved wet clutch. For evaluating the analytical model performance, numerical simulations were conducted using two open-source CFD codes: OpenFOAM and NEK5000; the latter can perform DNS. Besides, the two-phase flow was simulated with the OpenFOAM code. Two series of experimental data from previous studies were used to validate the numerical results.

Firstly, DNS is performed to obtain accurate results for the fluid flow in the wet clutch, regardless of the flow regime. Afterward, the presence of turbulence in the flow is investigated. This investigation proved that no sign of turbulence was found in the flow. A comparison between the steady-state laminar and DNS simulations confirmed the reliability of the laminar CFD model for further investigations. The CFD model was then used to evaluate the accuracy of the hydraulic diameter model in the single-phase condition. The predicted values of the model were approximately 50% closer to the numerical results of Pahlovy's model.

The difference between the analytical and numerical values was at most 8%, which is reasonable. After ensuring the good performance of the model in the single-phase condition, an approach similar to the model of Pahlovy et al. (12) was suggested for extending the hydraulic diameter model to the two-phase flow, resulting in a correlation for the oil volume fraction and drag torque in two-phase condition. Several CFD simulations were performed to validate the results obtained with the generalized hydraulic diameter model, which exhibited good agreement. Therefore, a revised version of the hydraulic diameter model has been presented. With the analytical model extended to the two-phase flow, the calculations can be performed more quickly, allowing more design iterations.

Even if analytical models -such as the model presented in this study- facilitate the calculation of drag torque and critical speed compared to experiment and CFD, they are not without limitations. For example, it is known that the geometry of the oil inlet and outlet influences the drag torque (10). The value of the drag torque differs significantly when oil is injected into the clutch and when the clutch is deeply lubricated. Since radial grooves are simple in design and construction, they have been the most studied in the literature and most analytical models have been extracted for this type of groove. However, there are other types of grooves that are widely used in industry and automotive applications and can be studied analytically. According to these issues, some potential topics for future studies include examining the impact of different clutch groove patterns on performance, such as inclined, sunburst, waffle-shape, and conical patterns, through numerical and analytical analysis. Besides, the concept of hydraulic diameter in the clutch can be modified and extended to various groove patterns to achieve more accurate results. Additionally, a new groove pattern, similar to the flow streamlines -suggested in some recent studies- can be

investigated to obtain its performance in single-phase and two-phase flows through experiments and CFD.

DISCLOSURE STATEMENT

The authors report there are no competing interests to declare.

NOMENCLATURE

A	Area (m^2)	Z	Axial direction (m)
$\vec{g}$	Gravitational acceleration (m/s^2)	α	Volume fraction
H	Groove height (mm)	θ	Tangential direction (rad)
h	Gap clearance (mm)	ϑ	Temperature (℃)
k	Turbulent kinetic energy (m^2/s^2)	μ	Dynamic viscosity (Pa.s)
N	Number of grid elements	ν	Turbulent kinematic viscosity (m2/s)
n	Number of grooves	ρ	Density (kg/m^3)
P	Pressure (Pa)	σ	surface tension (N/m)
Q	Volumetric flow rate (L/min)	φ	Contact angle (rad)
R_1	Inner radius (mm)	ω	Rotational speed (rad/s)
R_2	Outer radius (mm)		
Re	Reynolds number		
Re_L	Turbulent Reynolds number		
r	Radius (m)		
T	Drag torque (N.m)		

t	Time (s)
$\vec{U}$	Velocity vector (m/s)
W	Groove width (mm)

APPENDIX: Description of the hydraulic model generalization to two-phase condition

Based on Leister et al. (13), the Eq. (A.1) defines the pressure distribution in the radial direction in the clutch. It should be noted that the pressure gradient in the circumferential and axial directions is assumed negligible, the former due to the assumption of symmetric flow around the z-axis and the latter because of the $\frac{h}{R} \ll 1$ and the variation of the parameters in the axial direction is very small compared to the radial direction. Subsequently, this equation may be integrated in terms of r as below:

$$\frac{dp}{dr} = -\frac{6\mu Q}{\pi h^3 r} + \frac{3\rho r\omega^2}{10} \quad \text{(A.1)}$$

$$\int_{R_1}^{r} \frac{dp}{dr} dr = \int_{R_1}^{r} \left(-\frac{6\mu Q}{\pi h^3 r} + \frac{3\rho r\omega^2}{10}\right) dr \quad \text{(A.2)}$$

$$P(r) - P(R_1) = -\frac{6\mu Q}{\pi h^3} Ln(\frac{r}{R_1}) + \frac{3\rho\omega^2}{20}(r^2 - {R_1}^2) \quad \text{(A.3)}$$

The above equation can be used to explicitly calculate the pressure at each radius in the flow domain.

Afterward, we consider the simplifying assumption of Pahlovy et al. (12) . They assumed that by defining a critical radius, r_0, the flow domain is filled with oil from R_1 to r_0 and with air from r_0 to R_2. Fig. A1 shows a schematic of this assumption.

$$\alpha = \frac{r_0^2 - R_1^2}{R_2^2 - R_1^2} \tag{A.4}$$

It is important to note that this assumption is not physically true, because the experiments show that the distribution of the two phases is completely heterogeneous.

At the interface of air and oil, there should be a pressure drop that is balanced by the surface tension term. If the inner and outer boundary of critical radius, r_0, is shown by ${r_0}^+$ and ${r_0}^-$, the pressure drop can be written as:

$$\mathrm{P}({r_0}^+) - \mathrm{P}({r_0}^-) = \frac{2\sigma cos\varphi}{h} \tag{A.5}$$

where σ is the surface tension and φ is the contact angle. Putting ${r_0}^-$ in equation **Error! Reference source not found.** gives:

$$P(r_0^-) - P(R_1) = -\frac{6\mu Q}{\pi h^3} Ln(\frac{r_0^-}{R_1}) + \frac{3\rho\omega^2}{20}(r_0^{-2} - {R_1}^2) \tag{A.6}$$

Substituting Eq. (A.5) into Eq. (A.6) gives:

$$P(r_0^+) - P(R_1) = -\frac{6\mu Q}{\pi h^3} Ln\left(\frac{r_0^-}{R_1}\right) + \frac{3\rho\omega^2}{20}\left(r_0^{-2} - {R_1}^2\right) - \frac{2\sigma cos\varphi}{h} \tag{A.7}$$

Now the pressure value at the beginning of the air phase with consideration of surface tension is achieved. There are a lot of empirical and theoretical relations to measure the surface tension coefficient in terms of temperature and other thermophysical parameters in literature. Still, because the oil used in this study is identical to the one used in (10-11), the equation for surface tension coefficient at the interface between air and oil is given as follows (10):

$$\sigma = -8.444 \times 10^{-5}\vartheta_{oil} + 0.02992 \quad \text{(A.8)}$$

where ϑ_{oil} is the temperature of the oil and taken at 30℃. Pahlovy et al (12) claimed that at the equilibrium condition, the pressure at the beginning of the air layer is equal to the pressure at the entry of the clutch domain. Regarding this assumption, the left-hand side of Eq. (A.7) must be equal to zero. If the small difference between r_0^- and r_0 is neglected, the r_0^- can be substituted with r_0. Therefore, the critical radius can be obtained by solving the Eq. **Error! Reference source not found.**. Note that this equation must be solved by numerical methods and cannot be solved straightly for r_0.

$$-\frac{6\mu Q}{\pi h^3} Ln\left(\frac{r_0}{R_1}\right) + \frac{3\rho\omega^2}{20}\left({r_0}^2 - {R_1}^2\right) - \frac{2\sigma cos\varphi}{h} = 0 \quad \text{(A.9)}$$

Computing the oil volume fraction from Eq. (A.4) and multiplying that by Eq. (9) provides the analytical drag torque value as:

$$T = \frac{\alpha\pi\mu\omega}{2h_{eq}}\left({R_2}^4 - {R_1}^4\right) \quad \text{(A.10)}$$

As mentioned before, numerical investigations proved that the aforementioned equations have a reasonable accuracy in predicting the drag torque value in two-phase condition. But there are some deviations at the beginning of the aeration between numerical and analytical results. One could note that the onset of aeration occurs in a range of rotational speeds, not only in a specific point (10). However, the derived model considers a particular speed as the limit between two conditions: Fully single-phase and fully two-phase flow. The difference between analytical and numerical results around the critical speed could be due to this fact and needs to be investigated in future works.

REFERENCES

(1) Y. Kato, “Fuel Economy Improvement Through Tribological Analysis of the Wet Clutches and Brakes of an Automatic Transmission,” Proc. JSAE, 1993.

(2) C. R. Aphale, W. W. Schultz, and S. L. Ceccio, “The Influence of Grooves on the Fully Wetted and Aerated Flow Between Open Clutch Plates,” J. Tribol. vol. 132, no. January, pp. 1–7, 2010.

(3) H. Hashimoto, S. Wada, and Y. Murayama, “The Performance of a Turbulent-Lubricated Sliding Bearing Subject to Centrifugal Effect,” Trans. Jpn. Soc. Mech. Eng. Ser. C, vol. 49, no. 446, pp. 1753–1761, 1984.

(4) H. Kitabayashi, C. Y. Li, and H. Hiraki, “Analysis of the Various Factors Affecting Drag Torque in Multiple-Plate Wet Clutches,” SAE Technical Paper 2003-01-1973, 2003.

(5) Y. Yuan, E. A. Liu, J. Hill, and Q. Zou, “An improved hydrodynamic model for open wet transmission clutches,” *J. Fluids Eng. Trans. ASME*, vol. 129, no. 3, pp. 333–337, 2007.

(6) S. Iqbal, F. Al-Bender, B. Pluymers, and W. Desmet, “Mathematical Model and Experimental Evaluation of Drag Torque in Disengaged Wet Clutches,” ISRN Tribol., vol. 2013, pp. 1–16, 2013.

(7) W. Wu, Z. Xiong, J. Hu, and S. Yuan, “International Journal of Heat and Mass Transfer Application of CFD to Model Oil–Air Fow in a Grooved Two-Disc System,” Int. J. Heat Mass Transf., vol. 91, pp. 293–301, 2015.

(8) K. Guo, “Study on Aeration for Disengaged Wet Clutches Using a Two-Phase,” J. Fluids Eng. vol. 132, no. November 2010, pp. 1–6, 2018.

(9) P. Wang, N. Katopodes, and Y. Fujii, “Two-Phase MRF Model for Wet Clutch Drag Simulation,” SAE Int. J. Engines, vol. 10, no. 3, 2017.

(10) T. Neupert, E. Benke, and D. Bartel, “Tribology International Parameter Study on the Influence a Radial Goove Design on the Drag Torque of Wet Clutch Discs in Comparison with Analytical Models,” Tribol. Int., vol. 119, no. November 2017, pp. 809–821, 2018.

(11) T. Neupert and D. Bartel, “High-Resolution 3D CFD Multiphase Simulation of the Flow and the Drag Torque of Wet Clutch Discs Considering Free Surfaces,” Tribol. Int., vol. 129, pp. 283–296, 2019.

(12) S. A. Pahlovy, S. F. Mahmud, M. Kubota, M. Ogawa, and N. Takakura, “Prediction of Drag Torque in a Disengaged Wet Clutch of Automatic Transmission by Analytical Modeling,” Tribol. Online, vol. 11, no. 2, pp. 121–129, 2016.

(13) R. Leister, A. F. Najafi, D. Gatti, J. Kriegseis, and B. Frohnapfel, “Non-Dimensional Characteristics of Open Wet Clutches for Advanced Drag Torque and Aeration Predictions,” Tribol. Int., p. 106442, 2020.

(14) R. Leister, T. Fuchs, P. Mattern, and J. Kriegseis, “Flow-Structure Identification in a Radially Grooved Open Wet Clutch By Means of Defocusing Particle Tracking Velocimetry,” Exp. Fluids, vol. 62, no. 2, pp. 1–14, 2021.

(15) R. Leister, A. F. Najafi, J. Kriegseis, B. Frohnapfel, and D. Gatti, “Analytical Modeling and Dimensionless Characteristics of Open Wet Clutches in Consideration of Gravity,” Forsch. im Ingenieurwesen/Engineering Res., vol. 85, no. 4, pp. 849–857, 2021.

(16) C. Sax *et al.*, “Fluid-mechanical evaluation of different clutch geometries based on

experimental and numerical investigations," *Forsch. im Ingenieurwesen/Engineering Res.*, vol. 87, no. 4, pp. 1297–1306, 2023.

(17) L. Zhang, H. Zhou, P. Zhang, C. Wei, N. Ma, and Y. Yan, "Research on high-speed drag torque characteristics of wet clutches based on mechanism and data-driven approach," *Nonlinear Dyn.*, pp. 0–33, 2024.

(18) L. Zhang, C. Wei, and J. Bin Hu, "Model for the prediction of drag torque characteristics in wet clutch with radial grooves," *Proc. Inst. Mech. Eng. Part D J. Automob. Eng.*, vol. 233, no. 12, pp. 3043–3056, 2019.

(19) L. Pointner-Gabriel, K. Voelkel, H. Pflaum, and K. Stahl, "A methodology for data-driven modeling and prediction of the drag losses of wet clutches," *Forsch. im Ingenieurwesen/Engineering Res.*, vol. 87, no. 2, pp. 555–570, 2023.

(20) L. Pointner-Gabriel, M. Steiner, K. Voelkel, and K. Stahl, "Using Gaussian process regression for building a data-driven drag loss model of wet clutches," *Tribol. Int.*, vol. 198, no. May, 2024.

(21) S. B. Pope, "Turbulent flows." IOP Publishing, 2001.

(22) D. C. Wilcox, Turbulence Modeling for CFD, DCW industries La Canada, 3rd Edition, 2006.

(23) A. T. Patera, "A spectral element method for fluid dynamics: Laminar flow in a channel expansion," *J. Comput. Phys.*, vol. 54, no. 3, pp. 468–488, 1984.

(24) E. Tuliszka-Sznitko, A. Zieli´nski, and Z. Zieli´nski, "DNS/LES of Transitional Flow in Rotating Cavity," International J. Transport Phenomena , no. 3, 2008.

(25) E. Tuliszka-Sznitko, W. Majchrowski, and K. Kiełczewski, “Investigation of Transitional and Turbulent Heat and Momentum Transport in a Rotating Cavity,” Int. J. Heat Fluid Flow, vol. 35, pp. 52–60, 2012.

(26) M. Lygren and H. I. Andersson, “Turbulent flow Between a Rotating and a Stationary Disk,” J. Fluid Mech., vol. 426, pp. 297–326, 2001.

(27) E. Tuliszka-Sznitko and W. Majchrowski, “LES and DNS of the Flow with Heat Transfer in Rotating Cavity,” Comput. Methods Sci. Technol., vol. 16, no. 1, pp. 105–114, 2010.

(28) V. Michelassi, J. Wissink, and W. Rodi, “Analysis of DNS and LES of Flow in a Low Pressure Turbine Cascade with Incoming Wakes and Comparison with Experiments,” Flow, Turbul. Combust., vol. 69, no. 3–4, pp. 295–329, 2002.

(29) D. Liu, W. Tang, J. Wang, H. Xue, and K. Wang, “Comparison of Laminar Model, RANS, LES and VLES for Simulation of Liquid Sloshing,” Appl. Ocean Res., vol. 59, pp. 638–649, Sep. 2016.

(30) E. R. Hawkes and J. H. Chen, “Comparison of Direct Numerical Simulation of Lean Premixed Methane-air Flames With Strained Laminar Flame Calculations,” Combust. Flame, vol. 144, no. 1–2, pp. 112–125, 2006.

(31) Z. Jozefik, A. R. Kerstein, H. Schmidt, S. Lyra, H. Kolla, and J. H. Chen, “One-Dimensional Turbulence Modeling of a Turbulent Counterflow Flame With Comparison to DNS,” Combust. Flame, vol. 162, no. 8, pp. 2999–3015, 2015.

(32) A. P. Morse, “Application of a low Reynolds Number k-∈ Turbulence Model to High-Speed Rotating Cavity Flows,” Proc. ASME Turbo Expo, vol. 1, 1989.

(33) A. V. Dmitrenko, “Determination of Critical Reynolds Number for the Flow Near a Rotating Disk on the Basis of the Theory of Stochastic Equations and Equivalence of Measures,” Fluids, vol. 6, no. 1, 2020.

(34) P. R. N. Childs, Rotating Flow, Elsevier, 2011

(35) E. Crespo Del Arco, E. Serre, P. Bontoux, and B. E. Launder, Stability, transition and turbulence in rotating cavities, vol. 41. 2005.

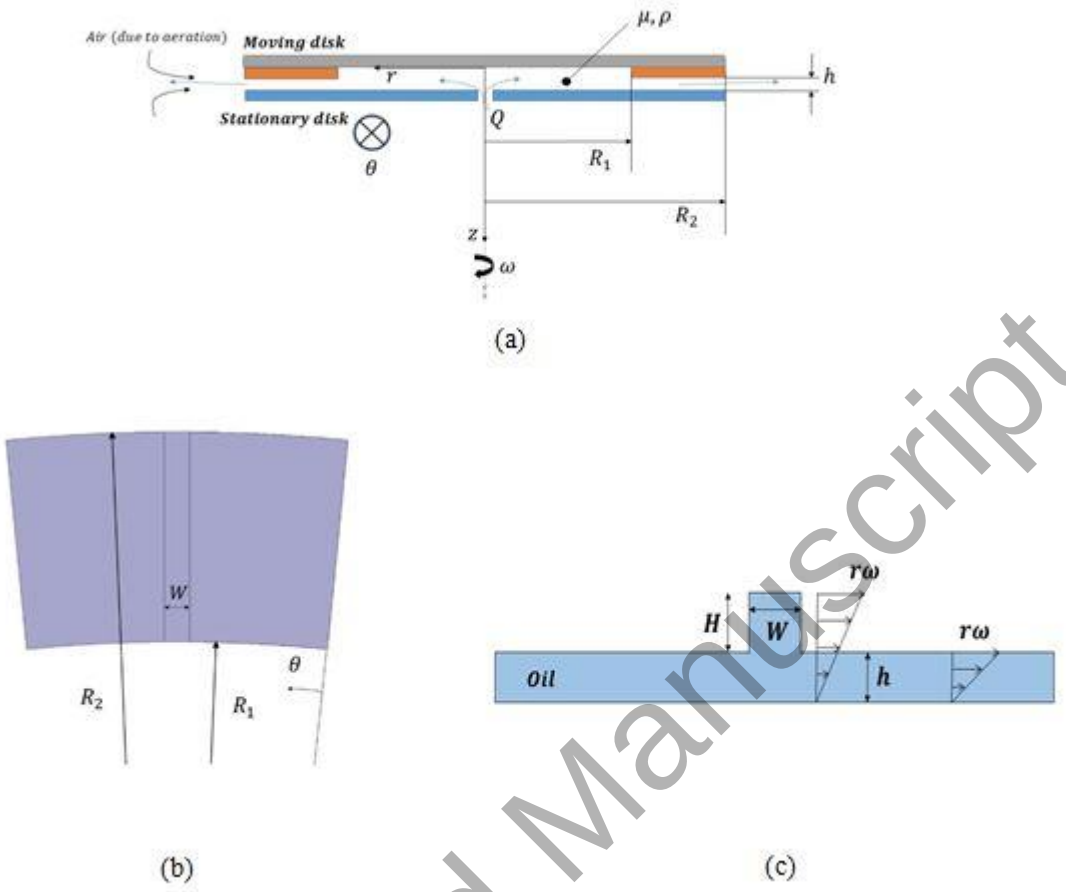

Fig. 1. A view of the computational domain with geometric parameters: a) Sketch of a non-grooved wet clutch with all geometric parameters, b) Top View, c) Front view

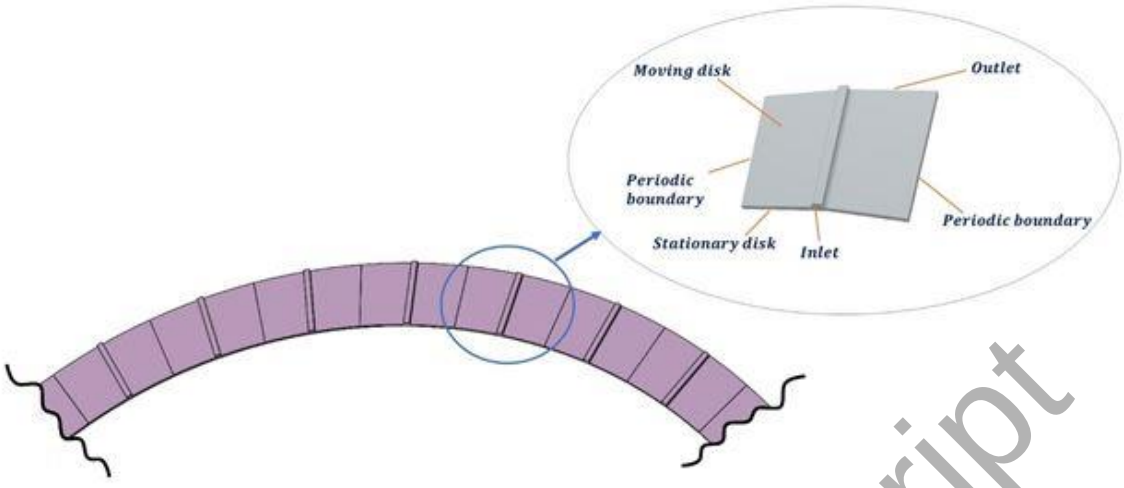

Fig. 2. A sector of the whole clutch with radial grooves (Case 1) with the definition of the boundary condition

Fig. 3. Computational grids

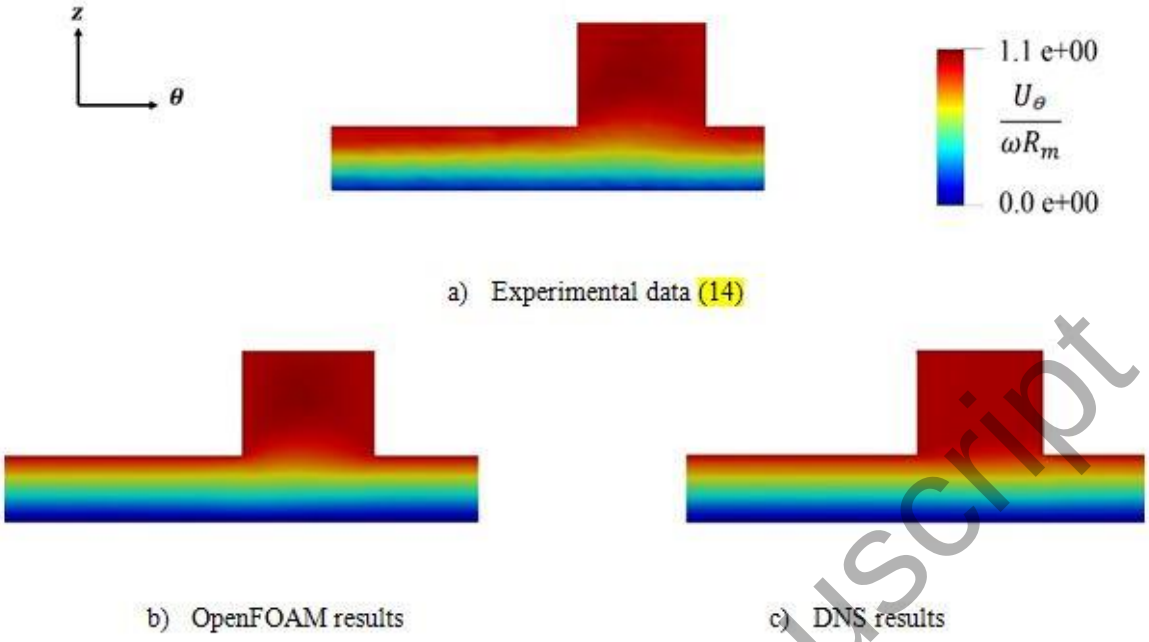

Fig. 4. Numerical and experimental contours of non-dimensionalized tangential velocity

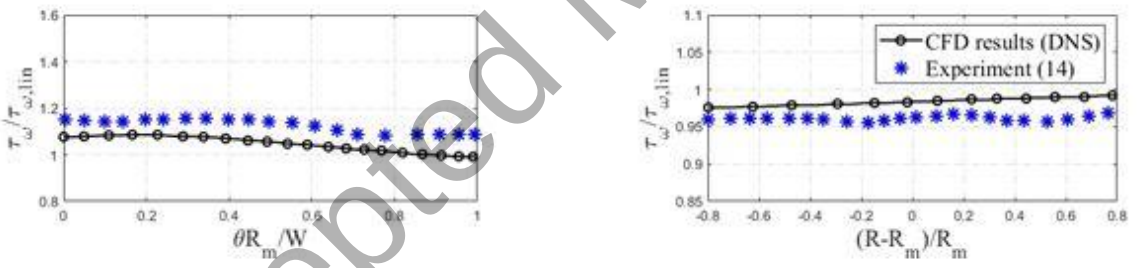

a) Non-dimensionalized wall shear stress in terms of the non-dimensionalized circumferential direction

b) Non-dimensionalized wall shear stress in terms of the non-dimensionalized radius in the middle of the groove ($\theta = 5.625°$)

Fig. 5. Validation of NEK5000 results with experiment (14)

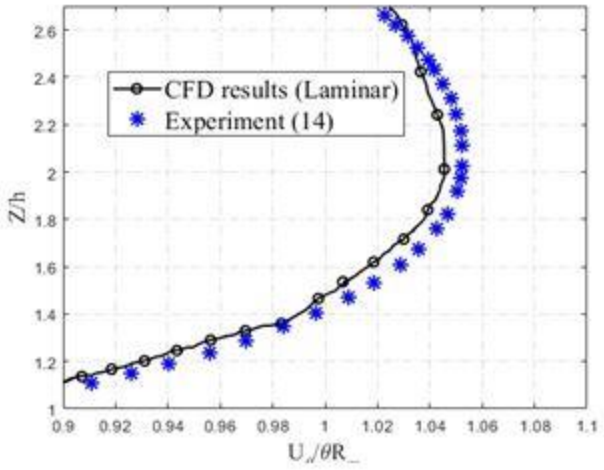

Fig. 6. Non-dimensionalized tangential velocity in terms of non-dimensionalized axial coordinate by OpenFOAM and experiment (14) for $\frac{\theta R_m}{W} = 0.5$

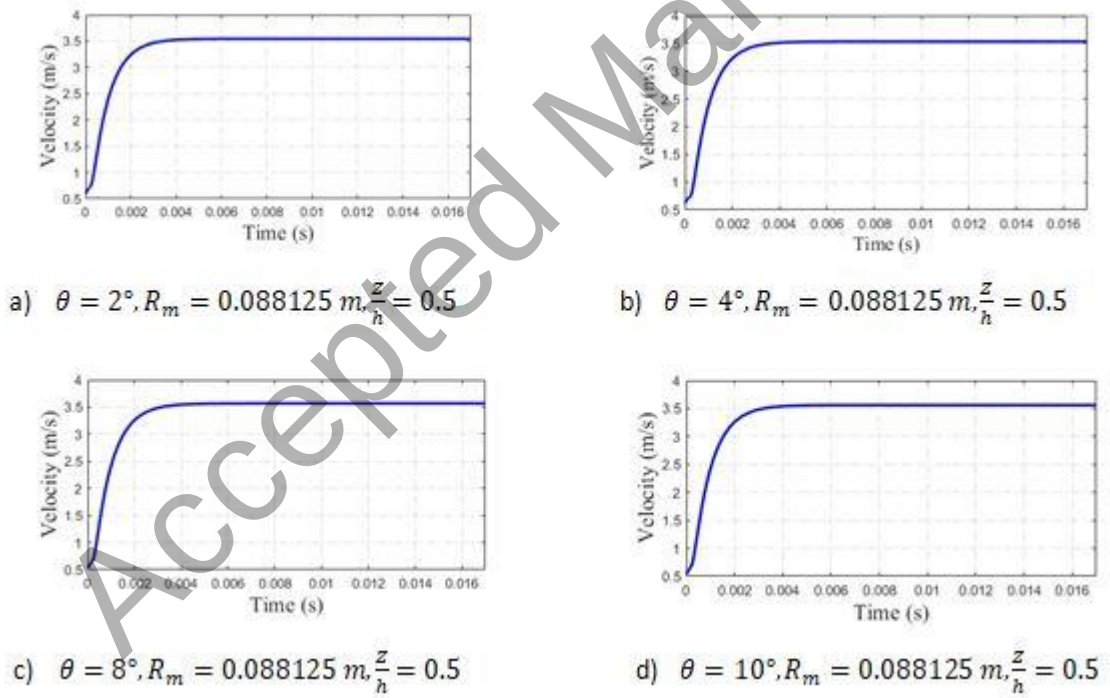

Fig. 7. Variation of velocity magnitude in 4 arbitrary locations in terms of time

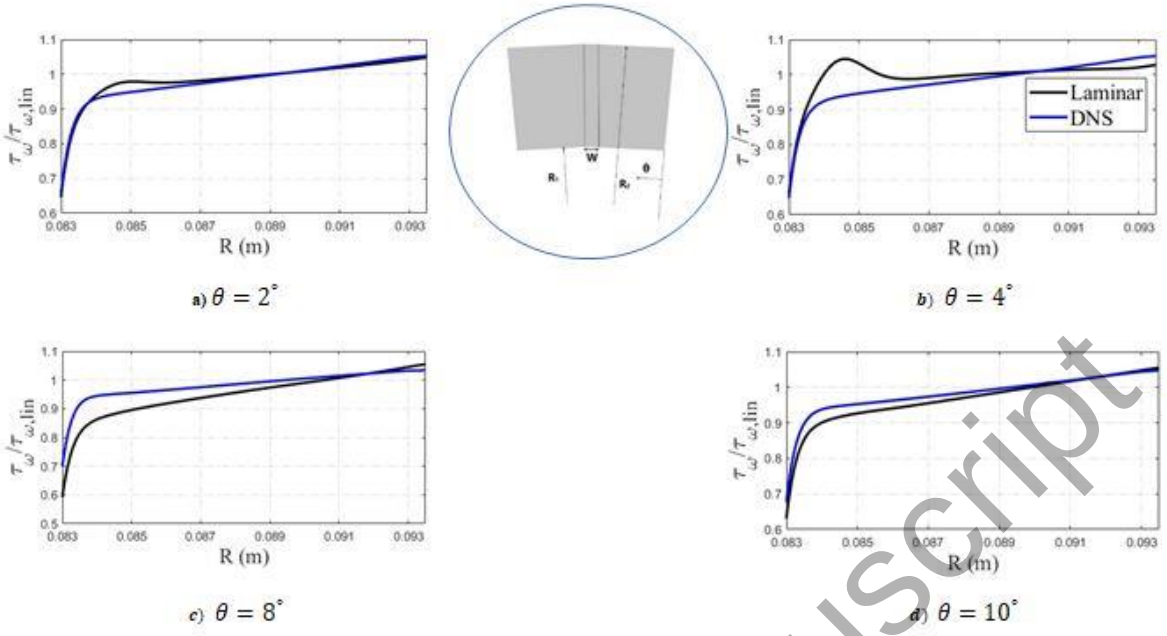

Fig. 8. Non-dimensionalized wall shear stress w.r.t the different clutch radii for ω = 80 rad/s

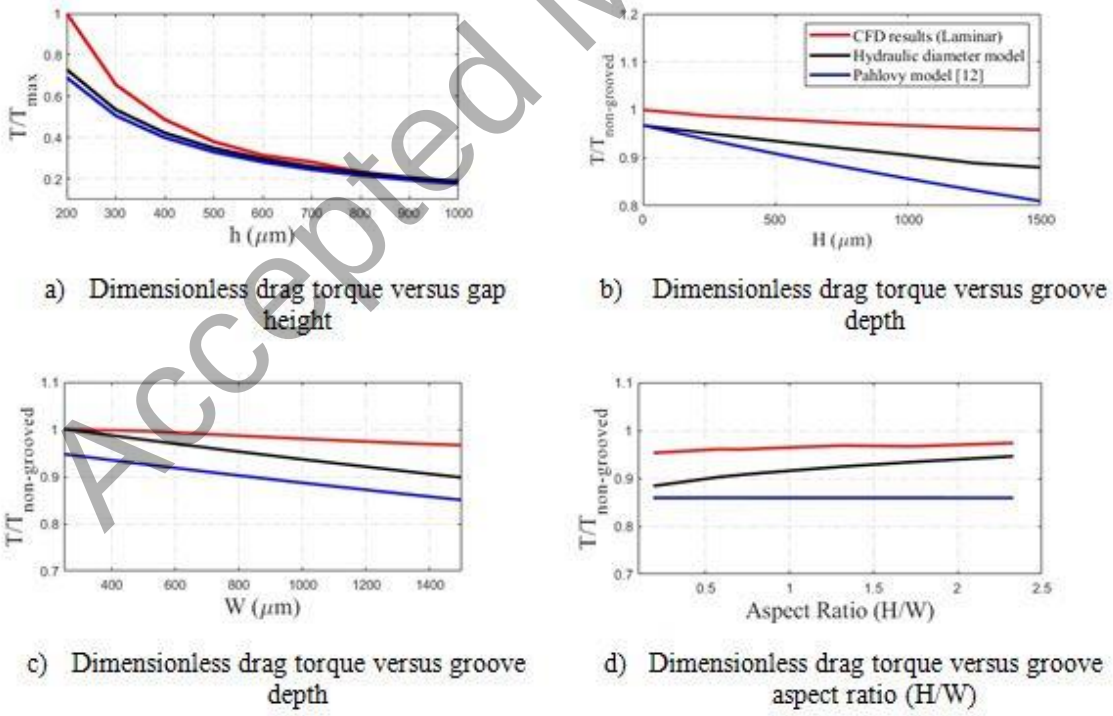

Fig. 9. Comparison between results obtained from simulation and two analytical models

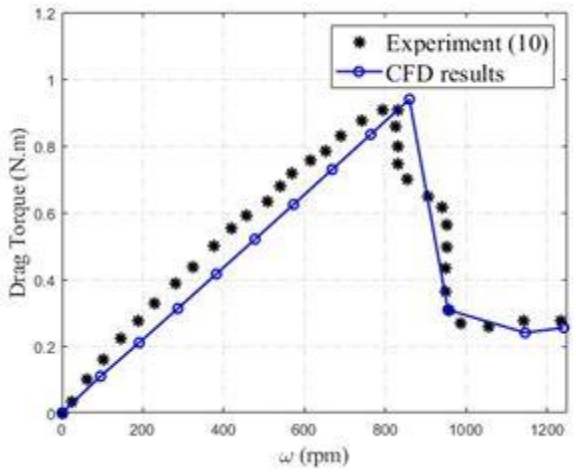

Fig. 10. Comparison between numerical and experimental results (10) for validating the two-phase simulation

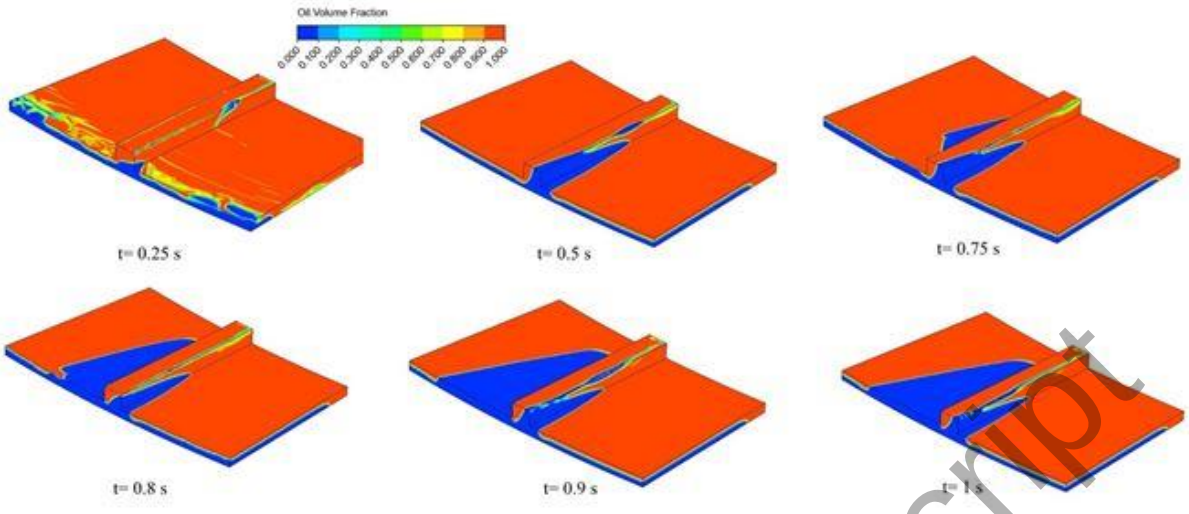

a) Contours of oil volume fraction during the simulation time at ω=100 rad/s and Q=3 L/min

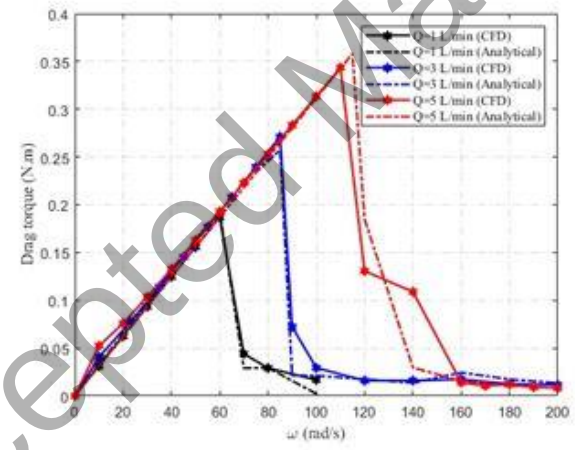

b) Drag torque curves obtained from CFD simulations and two-phase hydraulic diameter model

Fig. 11. Summary of simulation results for the two-phase flow condition of Case 1

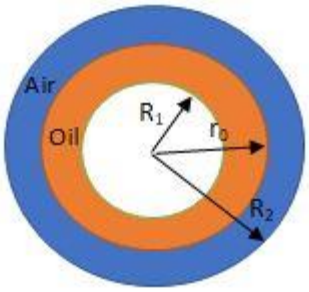

Fig. A1. Schematic of the Pahlovy's assumption for oil volume fraction (12)

Table 1. Geometrical parameters of the wet clutches considered

Quantity	Symbol	Case 1 (14)	Case 2 (10)
Groove depth [mm]	H	0.6	0.6
Groove width [mm]	W	1.35	1.5
Inner radius [mm]	R_1	82.5	67.5
Outer radius [mm]	R_2	93.75	84.25
Number of grooves	N	32	60
Gap clearance [mm]	h	0.6	0.15

Table 2. Comparison of simulation outputs between two different CFD methods

Solver	Flow regime model	Rotational speed (rad/s)	Drag torque (N.m)
OpenFOAM	Laminar	23	0.07836
NEK5000	DNS	23	0.07984
OpenFOAM	Laminar	80	0.2552
NEK5000	DNS	80	0.2577

Table 3. Comparison between numerical and theoretical critical velocities for the two-phase condition

$Q\ (L/min)$	Rotational speed (rad/s)		Difference
	Equation (11)	Numerical	
1	47.7	60	20%
3	82.55	85	2.9%
5	114.97	110	4.5%